Journal of Analytical and Applied Pyrolysis 113 (2015) 499–507

Contents lists available at ScienceDirect

Journal of Analytical and Applied Pyrolysis

journal homepage: www.elsevier.com/locate/jaap

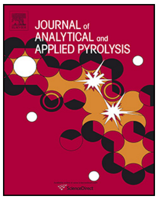

# Study on pyrolysis behaviors of non-woody lignins with TG-FTIR and Py-GC/MS

Lei Chen[a], Xianhua Wang[a,*], Haiping Yang[a], Qiang Lu[b,**], Di Li[a], Qing Yang[a], Hanping Chen[a]

[a] State Key Laboratory of Coal Combustion, Huazhong University of Science & Technology, Wuhan 430074, Hubei, PR China
[b] National Engineering Laboratory for Biomass Power Generation Equipment, North China Electric Power University, Beijing 102206, PR China

ARTICLE INFO

*Article history:*
Received 8 October 2014
Received in revised form 20 March 2015
Accepted 28 March 2015
Available online 30 March 2015

*Keywords:*
Non-woody lignin
Chemical structure
TG-FTIR
Py-GC/MS
Pyrolysis

ABSTRACT

To explore the potential values of lignins extracted from different agricultural wastes (e.g., walnut shell, wheat straw, cotton stalk, rice husk, bamboo, rape straw, corncob and peanut shell), pyrolysis behaviors of eight non-woody lignins were studied with TG-FTIR and Py-GC/MS. The TG-FTIR results indicated that the conversion of lignin and the evolution of main gaseous products were deeply influenced by the biomass species. Compared with the woody lignin, the phenylpropane unit present in the non-woody lignins would enhance the ability of condensation and lead to the formation of biochar. Also, differentiation of pyrolysis products was performed by Py-GC/MS. Corresponding to the classification of lignin types, the relative contents of syringol products from G type lignin were significantly less than those of the other two lignins (GS and HGS types). Compared with commercial alkali lignin (CAL, 6.7%), a high proportion of catechol type compounds was obtained from the peanut shell [37.5%] and cotton stalk [27.6%] lignins. Furthermore, the amount of styrene and 4-hydroxy-3-methoxystyrene was closely related to the content of hemicellulose in raw materials.

## 1. Introduction

Given the energy crisis and global warming, biomass has been regarded as a promising alternative to fossil fuels, due to its renewability and extensive distribution [1]. Lignin, one of the main biomass organic components, is the most abundant natural aromatic polymer composed of three phenylpropane units, i.e., p-hydroxyphenyl, guaiacyl and syringol units [2]. Because of its unique chemical structure, lignin is a feasible raw material for the production of valuable chemicals and medicines by tailoring molecules.

Pyrolysis is a promising technique to convert lignin into various monomers under different reaction conditions. Therefore, the pyrolysis characteristics of lignin have attracted increasing attention in recent years with the growing recognition that pyrolysis behavior is the foundation of selective pyrolysis, which can convert lignin into high value-added chemical products. Jakab et al. [3] investigated six woody lignin samples with thermogravimetry-mass spectrometry (TG–MS), and found the formation of water and formaldehyde were mainly ascribed to the decomposition of terminal $CH_2OH$ groups. Liu et al. [4] used a thermogravimetric analyzer coupled with a Fourier transform infrared spectrometry (TGA–FTIR) to study the pyrolysis behavior of fir and birch milled wood lignins and discussed the release profiles of the volatile products. Guo et al. [5] used a pyrolysis device to compare the pyrolysis characteristics of milled wood lignins obtained from Manchurian Ash (MA) and Mongolian Pine (MP), and found that a higher yield of bio-oil was produced in MA due to more methoxyl and free phenolic hydroxyl groups per C9 unit in MA than those in MP.

Compared with the thermal utilization of woody lignin, the exploration and application of non-woody lignin derived from agricultural wastes is rare at present [6]. Zhang et al. [7] studied the pyrolysis characteristic of prairie cordgrass (PCG) lignin and found PCG lignin was a good feedstock for producing bio-oil with high quality. Wild et al. [8] explored the bubbling fluidized bed for vaporisation of wheat straw lignin. Chen et al. [9] used FT-IR and Py-GC/MS to study the effects of the extraction method on the pyrolysis characteristic of lignin extracted from walnut shell. del Río et al. [10–12] employed comprehensive analytical techniques (Py-GC/MS, 2D-NMR, DFRC, etc.) to give a detailed elucidation of composition and structure of lignins extracted from coconut coir, wheat straw and elephant grass. In China, environmental pollution

---

* Corresponding author. Tel.: +86 027 87542417 8211; fax: +86 027 87545526.
** Corresponding author. Tel.: +86 10 61772063; fax: +86 10 61772032 801.
*E-mail addresses:* wxhwhhy@sina.com (X. Wang), qianglu@mail.ustc.edu.cn (Q. Lu).

http://dx.doi.org/10.1016/j.jaap.2015.03.018
0165-2370/

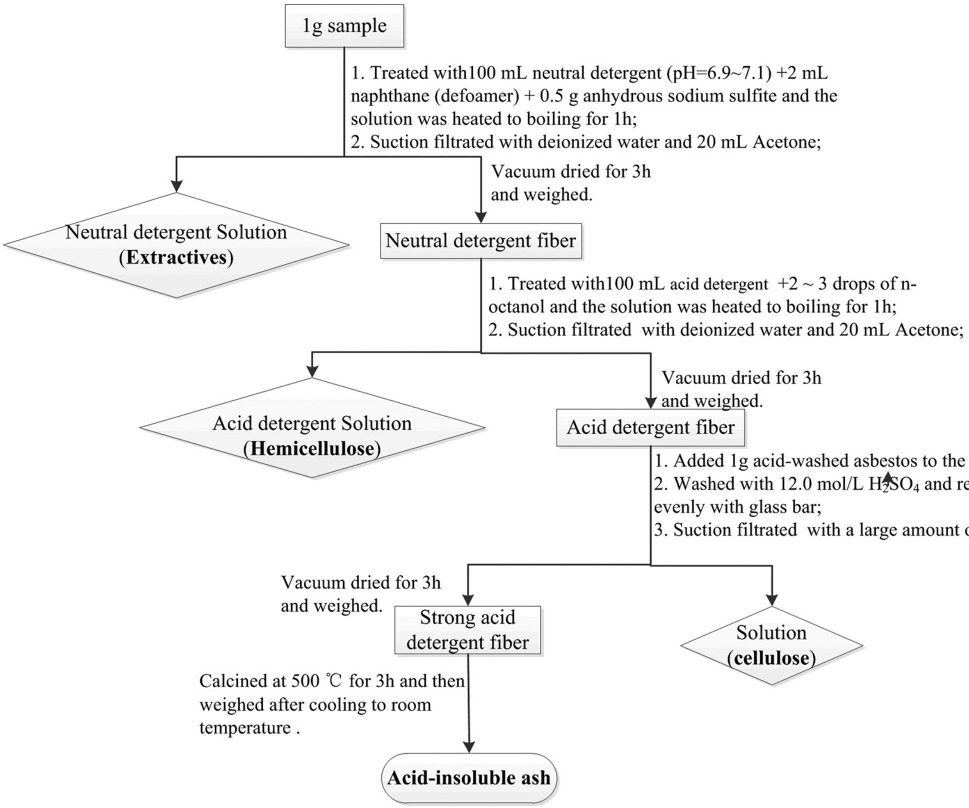

**Fig. 1.** Scheme for determination of fundamental organic compounds from various samples.

caused by situ-burning of common agricultural wastes, e.g., cotton stalk, rape straw, rice husk and corncob etc., promoted the Chinese Government to choose appropriate way to handle these materials. A good knowledge about chemical structures and pyrolysis characteristics of lignin isolated from non-woody plants is important for developing reasonable techniques to make full use of these residual wastes.

In order to estimate the value of these resources in thermal chemistry, it is necessary to investigate fully pyrolysis behavior of non-woody lignin extracted from different agricultural wastes. Hence, the thermal degradation characteristics of lignin derived from different generic crop residues were investigated using thermogravimetric analyzer with Fourier transform infrared spectroscopy (TG-FTIR), as well as pyrolysis-gas chromatography-mass spectrometry (Py-GC/MS). Then the effects of various chemical structures of lignin on the pyrolysis products were thoroughly analyzed. The purpose is to discover the probable useful pyrolysis characteristics of the raw materials. Such information is useful for the proper utilization of variant lignin resources.

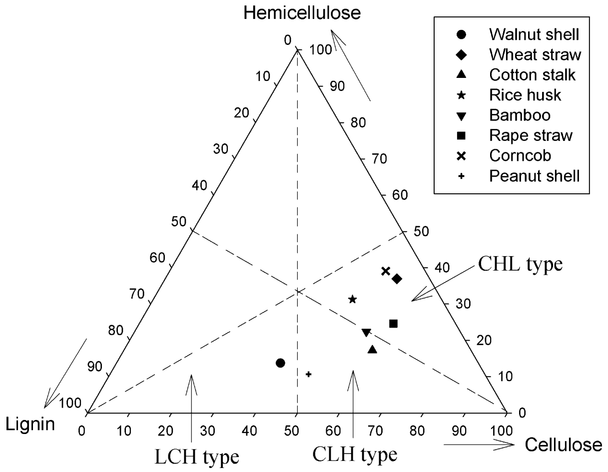

**Fig. 2.** The structural composition of the raw materials.

## 2. Materials and experimental methods

### 2.1. Materials preparation

Typical agricultural wastes including walnut shell, wheat straw, cotton stalk, rice husk, bamboo, rape straw, corncob and peanut shell were selected as feedstock in this study. The principal components of raw materials were analyzed with Van Soest's method, and the detailed procedure is shown in Fig. 1.

The lignin samples derived from variant biomass resources with Standard Klason procedure [13] were labeled as WASKL, WHSKL, CSKL, RHKL, BKL, RSKL, CCKL and PSKL orderly based on the sequence of the above mentioned materials. A CAL sample (Sigma–Aldrich) was used for comparison. Prior to each trial, the sample was dried at 105 °C overnight.

### 2.2. Experimental methods

FTIR of lignin samples were collected on KBr pellets (100 mg, 1 wt.%) using a Bruker Vertex 70 Fourier transform spectrometer. Spectra were obtained from 4000 $cm^{-1}$ to 400 $cm^{-1}$ at 4 $cm^{-1}$ resolution with 128 scans in triplicate and background spectra were collected in a KBr pellet. The spectra were processed by O.Faix's method [14] using OPUS software (see also the other studies [15,16]).

Thermogravimetric analysis was implemented using a TGA (Netzsch STA 449 F3 Germany) coupled with a FTIR (Bruker Equinox

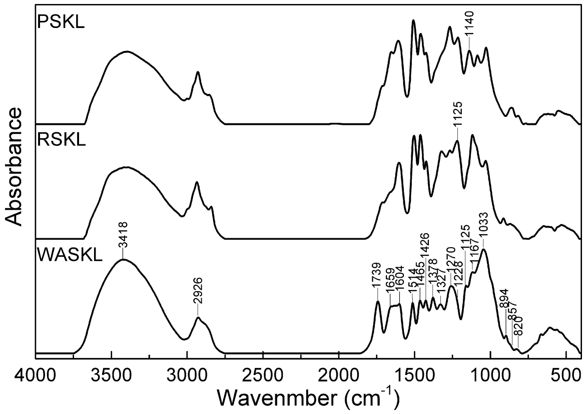

**Fig. 3.** The typical FTIR profiles of the G (PSKL), GS (RSKL) and HGS (WASKL) type lignins.

55). To eliminate the differences caused by heat and mass transfer, for each experiment, the sample weight was maintained at around 20 mg. The experimental setup was the same as that in our previous study [17].

To get further insights into how the chemical compositions of different lignin samples affected the properties of pyrolytic products, the pyrolysis experiments were conducted by a CDS 5200HP pyrolyzer (Chemical Data systems) with direct connection to a gas chromatography equipped with mass spectrometry (GC–MS, PerkinElmer Clarus560S). The details of the operational process were as follows: In each experiment, 0.2 mg sample was loaded into a quartz tube reactor. The temperature of the reactor was initially set at 50 °C, and then ramped to 600 °C for 10 s under helium gas (99.999%) at a nominal heating rate of 20 °C/ms. The pyrolysis vapor was directly transferred to the GC/MS and analyzed. The transfer line and GC injector temperatures were maintained at 300 °C. The chromatographic separation was achieved with a 30 m × 0.25 mm TR-35MS capillary column (0.25 μm film thickness). The oven temperature was initially maintained at 40 °C for 2 min, and then increased to 280 °C at a heating rate of 10 °C/min, then held for another 2 min. Helium at a constant flow rate of 1 mL/min was used as the carrier gas and the split ratio was 80:1. The separated compounds were then analyzed by the mass spectrometer, which was operated in electron ionization (EI) mode at the ionization energy of 70 eV. The mass spectra were obtained from m/z 20 to 400 with the scan speed of 500 Da/s. To ensure the good reproducibility of the above process, the experiments were performed at least five times on each lignin sample and the average results were used for analysis. Chromatographic peaks were identified through comparing the mass ions of each peak with NIST MS Library (2008) and the reported literature data from lignocellulosic material [18–21]. The chromatographic peak area of a specific compound is correlated linearly with its quantity, and its concentration can be reflected by the peak area ratio. The summed identified peak areas were normalized to 100% and the relative abundance of specific compound can be reflected by its peak area ratio.

## 3. Results and discussion

### 3.1. Elemental analysis and comparison of structural components

As shown in Table 1, cellulose, hemicellulose, lignin and extractives are the fundamental components of biomass. The proportion of the four components varies among different biomass types. According to theory of Vassilev et al. [22], biomass could be classified into six groups (CHL, CLH, HCL, LCH, HLC and LHC) based on the proportions of cellulose, hemicellulose and lignin. As demonstrated in Fig. 2, the results were as follows: (1) Lig–Cel–Hem (LCH) type: walnut shell; (2) Cel–Lig–Hem (CLH) type: cotton stalk and peanut shell; (2) Cel–Hem–Lig (CHL) type: wheat straw, rice husk, bamboo, rape straw and corncob.

**Table 1**
Component composition of the feedstocks on the dry basis (wt.%).

| | Extractives | Hemicellulose | Cellulose | Lignin | Acid-insoluble ash |
|---|---|---|---|---|---|
| Walnut shell | 1.85 | 13.32 | 37.92 | 45.74 | 1.17 |
| Wheat straw | 11.65 | 31.74 | 47.47 | 6.71 | 2.43 |
| Cotton stalk | 3.77 | 16.07 | 55.20 | 21.89 | 3.07 |
| Rice husk | 8.17 | 25.38 | 38.51 | 17.57 | 10.37 |
| Bamboo | 3.76 | 21.42 | 52.74 | 21.35 | 0.73 |
| Rape straw | 6.43 | 22.73 | 55.88 | 13.63 | 1.33 |
| Corncob | 5.63 | 36.79 | 48.43 | 8.82 | 0.33 |
| Peanut shell | 2.70 | 10.29 | 45.53 | 40.38 | 1.10 |

**Table 2**
Elemental composition of the lignin samples.

| Sample | Elemental analysis, wt.% (dry basis) | | | | Molar O/C | Molar H/C |
|---|---|---|---|---|---|---|
| | C | H | N | O[a] | | |
| CAL | 52.62 | 4.73 | 0.04 | 42.61 | 0.56 | 1.08 |
| WASKL | 52.32 | 5.91 | 0.22 | 41.55 | 0.60 | 1.36 |
| WHSKL | 53.98 | 4.27 | 1.03 | 40.72 | 0.57 | 0.95 |
| CSKL | 63.89 | 5.19 | 0.89 | 30.03 | 0.35 | 0.97 |
| RHKL | 40.94 | 3.56 | 0.50 | 55.00 | 1.01 | 1.04 |
| BKL | 60.64 | 4.90 | 0.68 | 33.78 | 0.42 | 0.97 |
| RSKL | 63.44 | 5.12 | 0.62 | 30.82 | 0.36 | 0.97 |
| CCKL | 60.48 | 4.93 | 1.37 | 33.22 | 0.41 | 0.98 |
| PSKL | 65.67 | 5.80 | 0.92 | 27.61 | 0.32 | 1.06 |

[a] The O content was determined by difference.

The results of ultimate analyses of these lignin samples are outlined in Table 2. The carbon contents of CSKL, BKL, RSKL, CCKL and PSKL were more than 60 wt.%, whereas the oxygen content was below 35 wt.%. RHKL contained the lowest carbon content (40.94 wt.%) and the highest oxygen content (55 wt.%) among the studied samples. The elemental compositions of WASKL and WHSKL samples were very similar to that of CAL.

### 3.2. FTIR spectroscopy analysis

The chemical structures of the lignin samples were characterized with FTIR, and the results are shown in Table 3 and Fig. 3. The spectra profiles exhibited typical lignin patterns [19], e.g., OH (3460–3412 cm$^{-1}$), CH (3000–2842 cm$^{-1}$), C═O (1738–1593 cm$^{-1}$) and C—H (925–832 cm$^{-1}$). However, the fingerprint region (1800–800 cm$^{-1}$) was composed of a group of complicated IR absorbance, which differed significantly in spectral intensity and distribution of peak positions [17]. These differences might be due to the different proportions of guaiacyl unit, syringyl unit and P-hydroxyphenyl unit in lignin.

Following O. Faix's theory [14], lignin could be classified into three types according to the peak positions in the spectra, namely G lignin, GS lignin and HGS lignin. Respected to the lignin samples involved here, CAL, RHKL and PSKL were G lignins with a peak at 1140 cm$^{-1}$ induced by aromatic C—H in-plane deformation, while the CSKL and RSKL belonged to GS lignins due to the vibration of aromatic C—H deformation of syringyl units and secondary alcohols, with a peak shown between 1128 cm$^{-1}$ and 1125 cm$^{-1}$. For WASKL, WHSKL, BKL, CCKL, although the presence of peaks at 1125 cm$^{-1}$, these samples fell into the category of HGS lignins, as the peaks appeared with a shoulder around 1167 cm$^{-1}$ which originated from C═O in ester groups (conj.).

The ratio of syringyl to guaiacyl (S/G) was an important indicator to distinguish the lignin sources and affect the utilization ways

**Table 3**
FT-IR analysis of the lignin samples.

| Range of maxima | Band assignment | Maxima at $cm^{-1}$, absorbance | | | | | | | | |
|---|---|---|---|---|---|---|---|---|---|---|
| Wavenumber/$cm^{-1}$ | | CAL | WASKL | WHSKL | CSKL | RHKL | BKL | RSKL | CCKL | PSKL |
| 3460–3412 | O—H stretching | 3435 | 3418 | 3414 | 3420 | 3422 | 3420 | 3422 | 3419 | 3420 |
| 3000–2842 | C—H stretch in methyl and methylene group | 2934 | 2926 | 2933 | 2935 | 2934 | 2933 | 2935 | 2935 | 2929 |
| | | | | 2849 | 2841 | 2844 | 2842 | 2841 | 2846 | 2855 |
| 1738–1709 | C=O stretch in unconjugated ketone, carbonyl and ester groups | | 1739 | 1720 | 1718 | 1717 | 1718 | 1711 | 1714 | 1717 |
| 1675–1655 | C=O stretching in conjugated p-subst. Aryl ketones | | 1659 | 1661 | 1657 | 1661 | 1657 | 1663 | 1655 | 1660 |
| 1605–1593 | Aromatic skeleton vibrations plus C—;O stretching; S>G: $G_{condensed}$>$G_{etherified}$ | 1595 | 1604 | 1597 | 1601 | 1604 | 1601 | 1603 | 1598 | 1600 |
| 1515–1505 | Aromatic skeleton vibrations (G > S) | 1507 | 1514 | 1506 | 1506 | 1506 | 1506 | 1504 | 1505 | 1506 |
| 1470–1445 | C—H deformations (asym in —$CH_3$ and—$CH_2$—) | 1462 | 1465 | 1461 | 1461 | 1461 | 1461 | 1460 | 1458 | 1459 |
| 1430–1422 | Aromatic skeleton vibrations combined with C—H in plane deformations | 1422 | 1426 | 1425 | 1423 | 1424 | 1425 | 1423 | 1422 | 1422 |
| 1370–1365 | Aliphatic C—H stretching in $CH_3$ and phen. OH | 1373 | 1378 | 1366 | 1372 | 1368 | | 1372 | 1370 | 1370 |
| 1330–1325 | Condensed S and G ring (G ring bound via position 5) | | 1327 | 1325 | 1326 | 1325 | 1332 | 1325 | 1325 | 1323 |
| 1270–1266 | G ring plus C + O stretching | 1266 | 1270 | 1269 | 1268 | 1270 | 1268 | 1270 | 1268 | 1269 |
| 1233–1214 | C—C + C—O + C=O stretching ($G_{condensed}$>$G_{etherified}$) | 1216 | 1230 | 1218 | 1215 | 1215 | 1218 | 1217 | 1215 | 1214 |
| 1166 | Typical for HGS lignins; C—O in ester groups (conj.) | | 1166 | 1167 | | | 1165 | | 1165 | |
| 1140 | Aromatic C—H in-plane deformation (typical of G unit; $G_{condensed}$>$G_{etherified}$) | 1138 | | | | 1140 | | | | 1140 |
| 1128–1125 | Typical of S unit; also secondary alcohol and C—O strt. | | 1125 | 1125 | 1125 | | 1128 | 1125 | 1126 | |
| 1110 | Aromatic C—H deformation of S units | | | | | | | 1110 | | |
| 1086 | C—O deformation in sec. alcohol and aliphatic ether | 1082 | 1086 | 1087 | 1091 | 1086 | 1098 | 1087 | 1087 | 1085 |
| 1035–1030 | Aromatic C—H in-plane deformation (G > S) plus C—O deform. in primary alcohols plus C—H stretching (unconjugated) | 1039 | 1033 | 1035 | 1031 | 1033 | 1033 | 1033 | 1035 | 1030 |
| 990–966 | —HC=CH—out -of-plane deform (trans) | | | 981 | | 966 | 974 | 970 | 985 | 970 |
| 925–915 | C—H out of plane (aromatic ring) | | | | 916 | | 915 | 914 | 925 | |
| 895–885 | C—H deformation vibration; $CH_2$ wagging | 856 | | | | | | | | |
| 858–853 | C—H out of plane in positions 2, 5 and 6 (G units) | | 857 | | 860 | | | 856 | | 858 |
| 835–834 | C—H out of plane in positions 2 and 6 (S units) | | | 835 | | | 834 | | 835 | |
| 832–817 | C–H out of plane in positions 2, 5 and 6 (G units) | 815 | 820 | 822 | 819 | | | 816 | | 817 |

G: Guaiacyl units;S: Syringyl units;H: P-hydroxyphenyl unit.

**Table 4**
The classification and *S*/*G* values of the lignin samples.

| Sample | Type | *S*/*G* | Sample | Type | *S*/*G* |
|---|---|---|---|---|---|
| CAL | G | 0.326 | WASKL | HGS | 0.77 |
| BKL | HGS | 1.9 | WHSKL | HGS | 0.676 |
| RSKL | GS | 1.25 | CSKL | GS | 0.905 |
| CCKL | HGS | 0.656 | RHKL | G | 0.613 |
| PSKL | G | 0.689 | | | |

of biomass, e.g., delignification [15,21]. The S/G ratios of the eight samples were determined by Sammons's methods and summarized in Table 4. From Table 4, the values varied from 0.326 to 1.9, among which the S/G ratio of BKL was the highest, which suggested that bamboo facilitated the isolation of lignin and possessed low-grade recalcitrance [6].

### 3.3. *Thermal analysis of the lignin samples*

The thermal decomposition characteristics of the lignin samples, including both plots of weight loss (in wt.%) and weight derivation rate (in wt.%/°C), are presented in Fig. 4. The first weight loss stage (80 °C–200 °C) was mainly caused by the evaporation of moisture and some organic constituents (including alkyl, alkene and carbonyl functional groups) [23,24]. The main weight loss occurred in the range of 300–600 °C. In contrast with CAL, the DTG curves of the Klason lignins seemed simple and the highest thermal velocities were concentrated at 365 °C (Fig. 4 (b)), which suggested that the temperature range for the devolatilization of Klason lignins was narrower than that of CAL. Moreover, the maximum degradation rates and final solid residue yields varied greatly across the samples. The maximum degradation rates of WASKL and CAL were 9.6 wt.%/°C and 5.0 wt.%/°C, respectively. As shown in Fig. 3 (b), the DTG curve of WASKL displayed an additional shoulder ( 300 °C), suggesting that WASKL had a superior degradation behavior. This could be a possible explanation for low charcoal residue from WASKL [25].

With respect to the charcoal yields, the least amount of charcoal residue (29.5 wt.%) was obtained from WASKL, whereas that obtained from RHKL was the highest (68.8 wt.%), which should be due to the differences in the contents of HGS units and the amounts of acid-insoluble ash of the lignin samples. This implied RHKL had the potential to be used for preparing biochar. Lignin, which was a heterogeneous polymer, contains ether bonds and C—C bonds to serve as the "bridge" of lignin monomers [26]. Faix et al. [25] pointed out that the rapture of thermolabile ester and ether bonds could lead to high degradability. Given the highest degradability of WASKL (with the least amount of charcoal residue), it was reasonable to infer that WASKL contained more thermolabile ester and ether bonds than the others. As previously mentioned, WASKL and RHKL belonged to HGS type and G type lignins, respectively. Besides, the S/G ratio of WASKL was 0.157 higher than that of RHKL. Kotake et al. [27] proposed that the quinone methide and radical pathway were important for polymerization and side-chain-conversion processes. Electro-positive carbons of quinone methide, which acted as an important intermediate of coniferyl alcohol, reacted with electro-negative aromatic and double bond carbons rather than the oxygen of the side-chain and the phenolic functional groups. The high condensation reactivity of coniferyl alcohol and its primary products led to the tendency to form charcoal in lignin pyrolysis. Additionally, compared with the ether bonds, condensed (C—C) linkages would be more stable during the pyrolysis process. This could explain why it was unlikely for the condensation products to occur secondary thermal cracking. [28].

Although the *S*/*G* values of CSKL, BKL and RSKL were higher than that of the WASKL, the latter had less charcoal residue left. Faix et al. [25] pointed out that H unit also showed a high tendency for condensation reactions. Furthermore, Liu et al. [29] conducted the pyrolysis experiments of two β-O-4 model polymers with each composed of H and G units, and found that charcoal residue left from the H type lignin model polymer was higher than that from the G type lignin model polymer. Hence, the presence of H unit in the non-woody lignin resulted in a more complicated pyrolysis behavior than the woody lignin. It suggested that the *S*/*G* values and the lignin types could not account for the differences in the charcoal yields to some extent, while these differences might be related to the diversity of the contents of H unit among the lignin samples.

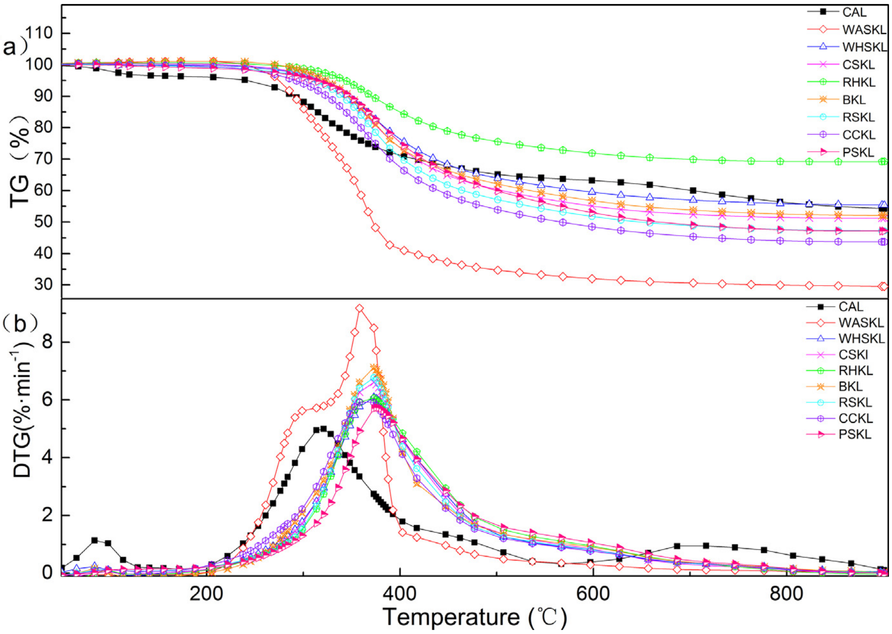

**Fig. 4.** TG (a) and DTG (b) curves of the lignin samples.

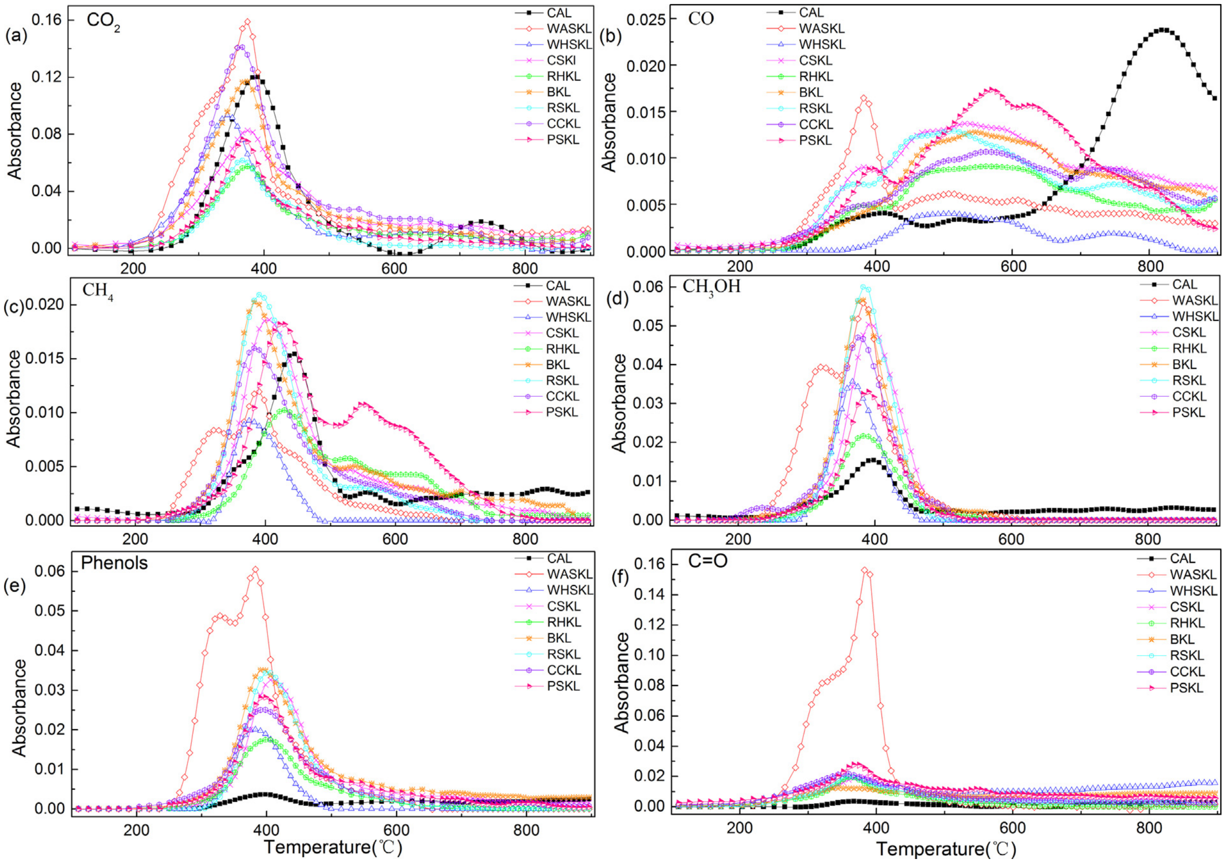

**Fig. 5.** FTIR profiles of the pyrolysis products evolving from the lignin samples.

### 3.4. Gas releasing property from pyrolysis of the lignin samples

As shown in Fig. 5(a–e), the wave numbers of FTIR peaks of six pyrolysis products as a function of temperature were as follows: $CO_2$ – 2358 cm$^{-1}$, CO – 2181 cm$^{-1}$, $CH_4$ – 3022 cm$^{-1}$, $CH_3OH$ – 1057 cm$^{-1}$, phenols – 1220 cm$^{-1}$ and carbohydrates containing carbonyl group – 1730 cm$^{-1}$ [17,30].

Thermal splitting of $CO_2$ from Klason lignins mainly occurred in the temperature region of 230–580 °C and all the releasing curves peaked at about 370 °C except for WHSKL (347 °C). Compared with $CO_2$, the releasing of CO appeared to be more complicated. The formation of CO below 400 °C was the consequence of the cleavage and conversion reactions of carboxyl, carbonyl, and ester groups in the side-chain of phenyl propane [25]. However, the evolution of CO in the temperature range of 550–660 °C might be ascribed to the thermal degradation of catechol/pyrogallol intermediate [31]. With the increase of temperature, the cracking of carbonyl and carboxyl functional groups from the primary tar components contributed to the formation of CO [32]. From Fig. 5(b), it can be observed that the releasing of CO from CAL occurred predominantly after 600 °C, while, that from non-woody Klason lignin was found mainly in a broad range from 300 °C to 800 °C, except for WASKL, from which a significant narrow peak was found between 300 °C and 420 °C with the maximum releasing of CO located at about 370 °C.

There are three main theories on the formation mechanism of $CO_2$. Kawamoto et al. [31] advocated that $CO_2$ was mainly produced by the intermediate products of $-OCH_3$ homolysis reaction and coke; another theory suggested that $CO_2$ resulted from cracking and reforming of carboxyl, carbonyl and ether groups in the phenylpropane side chains [3,30]. Besides, Pandey et al. [1] argued that $CO_2$ could be directly obtained by the demethoxylation reaction. As shown in Fig. 5 (a–f), the releasing of $CO_2$ was much earlier than those of other pyrolysis products. Therefore, $CO_2$ might be produced by the cracking of ether bonds and subsequent demethoxylation reaction in the phenylpropane side chains, which was different from the formation characteristic of CO, in contrast to previous studies [1,31].

With regard to the formation of $CH_4$ and $CH_3OH$, demethylation was the main source of $CH_4$, and the temperature of the principal peak of $CH_4$ releasing was widely distributed. WASKL displayed two peaks located at 320 °C and 390 °C. As shown in Fig. 5 (c), the temperatures of maximum release value were different and could be arranged in the order of HGS < GS < G. On the other hand, the release of $CH_4$ from PSKL (G type lignin) with the peaks located at 430 °C and 530 °C was a bit later than the other samples. Compared with $CH_4$, the releasing behaviors of $CH_3OH$ from various samples seemed very simple as 370–390 °C was the major temperature range for the highest thermal decomposition. Since the operational procedures were identical, the absorbance of specific gas had a linear relationship with its concentration [30,33]. As depicted in Fig. 5(d), the $CH_3OH$ concentrations from GS and HGS type lignins were obviously more than that from G type lignin. Meanwhile, a shoulder was found for $CH_3OH$ releasing from the WASKL, which indicated that the release of $CH_3OH$ might correspond with the superiority on the degradation process of WASKL. Asmadi et al. [34] proposed that the $-OCH_3$ homolysis and rearrangement led to the production of the $CH_4$. In addition, the evolution of $CH_3OH$ might be the byproduct of $-OCH_3$ rearrangement. Compared with the other volatile components, the temperature range of $CH_3OH$ releasing was narrow (300–500 °C) and was slightly larger than that of woody lignin [30].

As shown in Fig. 5(e), the releasing temperature range for phenols from pyrolysis of the studied non-woody lignins were very similar except for the WASKL with two peaks: the first one with a lower absorbance at 330 °C, and the second one at 380 °C with much higher absorbance. The formation of phenolic monomers and oligomers was mainly brought by the fragmentation of the ether cleavage and H-abstraction [28]. The gas-phase organics with C=O bond wwere important components of the volatiles. As shown in Fig. 5(f), carbonyl group obtained from WASKL was much higher than that of the other samples. Since the decarbonylation reaction was parallel to the H-abstraction from aldehyde-H, the aldehyde group acted as an H-donor to the radical species and inhibited the condensation reaction [32]. This could explain why WASKL showed lower charcoal residue than the other samples. Generally, aldehyde-H from the H-abstraction reaction played a more prominent role in the formation of the charcoal residue than the value of S/G. Furthermore, combined the superiority of lignin-rich and pyrolysis characteristic, walnut shell was a favorable resource for preparing aromatic bio-oil.

### 3.5. Py–GC/MS analysis

Table 5 and Fig. 6 lists the organic components released from fast pyrolysis of lignin samples with Py–GC/MS analysis. As shown in Table 5 and Fig. 6, the main organic species evolved out from fast pyrolysis of lignin were similar, they can be classified into five types: benzene, phenol, guaiacyl, syringol, and catechol types based on the chemical structure and main formation pathways during thermal degradation [24,35]. Nevertheless, the relative yields varied greatly, especially for phenol, syringol, catechol and their derivates (Fig. 7). For benzene and its derivatives, WHSKL showed the highest yield, whereas no obvious difference was observed for other lignin samples. Toluene, a major variant of benzene type product, was mainly generated from the decomposition of the intermediate of anisole. A larger amount of simple phenol and its derivatives, especially cresol, which were products of $OCH_3$ rearrangement [36], were generated from pyrolysis of WHSKL, RHKL, BKL and PSKL than that from WASKL, CSKL, RSKL, CCKL and CAL. In addition to the production from the cracking of p-hydroxyphenyl

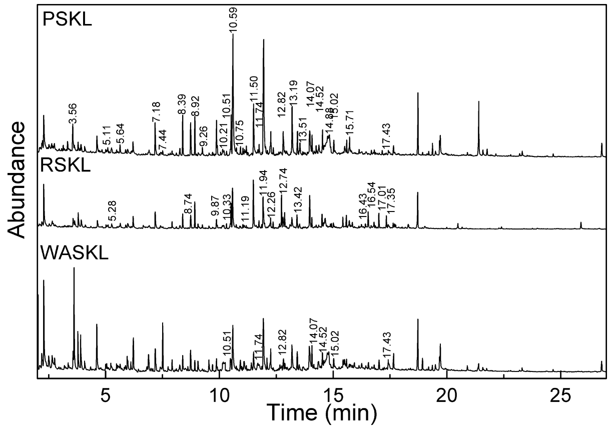

**Fig. 6.** Typical ion chromatograms from pyrolysis of the G, GS and HGS type lignins (peak identification referred to Table 5).

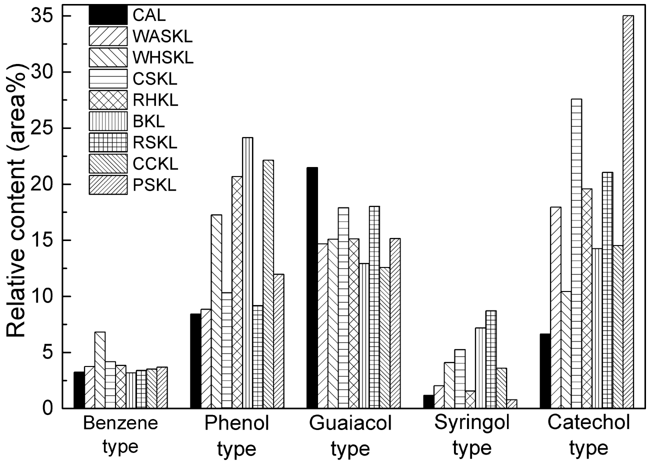

**Fig. 7.** Distributions of benzenes, phenols, guaiacols, syringols and catechols and their derivatives.

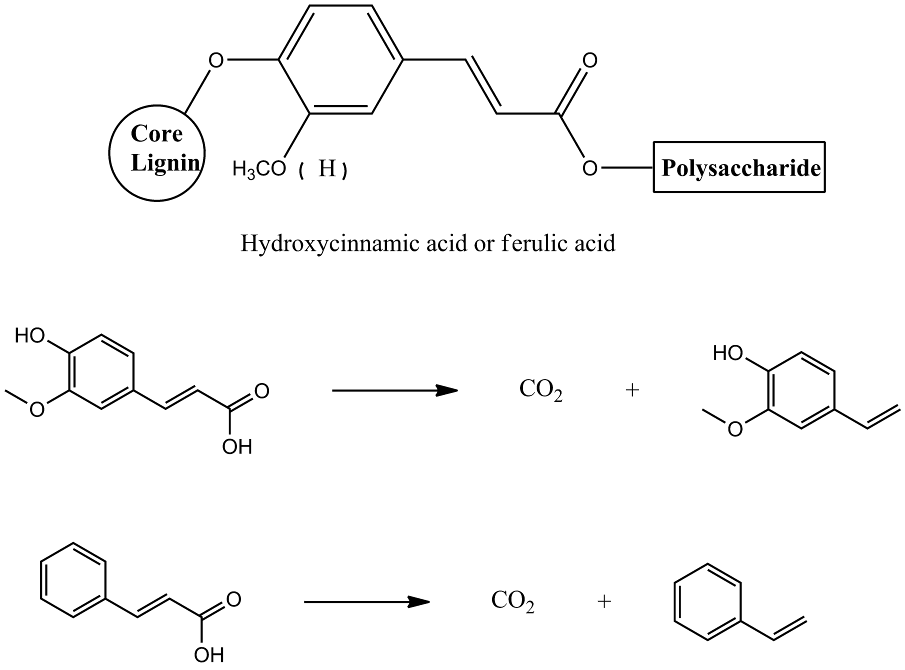

**Fig. 8.** The function and pyrolysis products of cinnamic acid bridges.

**Table 5**
The main identified products from fast pyrolysis of the lignin samples.

| NO. Benzene type | NO. Phenol type | NO. Guaiacol type (G) | NO. Syringol type (S) | NO. Catechol type (C) |
|---|---|---|---|---|
| 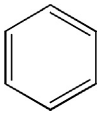 | 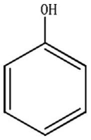 | 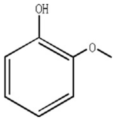 | 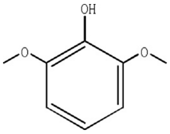 | 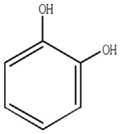 |
| Toluene (3.56)[a]<br>Ethylbenzene(5.11)<br>1,2-xylene(5.28)<br>Styrene(5.64) | Phenol(7.18)<br>Vinylphenol(7.44)<br>o-Cresol [8.39]<br>4-Methylphenol(8.74)<br>2,6-Dimethylphenol(9.26)<br>2,5-Dimethylphenol(9.87)<br>3,5-Dimethyl-phenol(10.21)<br>Mesitol(10.75)<br>m-Cresol,6-ethyl-(11.19) | Guaiacol(8.92)<br>2-Methoxy-6-methylphenol(10.33)<br>2-Methoxy-4-methylphenol(10.51)<br>4-Ethylguaiacol(11.74)<br>4-Hydroxy-3-methoxystyrene(12.26)<br>Eugenol(12.82)<br>Vanillin(13.42)<br>4-Propenylguaiacol(13.51)<br>cis-Isoeugenol(14.07)<br>Acetovanillone(14.52)<br>Methyl vanillate(14.88)<br>Vanillyl methyl ketone (15.02)<br>Vanillic acid hydrazide(15.71)<br>Homovanillic acid(16.43)<br>Coniferylaldehydel(17.43) | Syringol(12.74)<br>Syringaldehyde(16.54)<br>4-Allylsyringol(17.01)<br>Syringylethanone(17.35) | Catechol(10.59)<br>3-Methylcatechol(11.50)<br>4-Methylcatechol(11.94)<br>Ethylcatechol(13.19) |

Other compounds: acetic acid (1.85), methyl ester acetic acid(2.28), methyl valeraldehyde(3.80), 2-cyclopentenone(4.63), 2-hexene, (E)- (8CI)(6.00), cyclohexanone(6.21), 2-hydroxybenzaldehyde(8.28), pentanal (9.08), 1,2ethanediol,monobenzoate(10.13), 2-methoxybenzyl alcohol(10.17), 2-methoxy-6-methylphenol(10.33), phenyl vinyl ether(10.92), 3-methoxyphenol(11.04), 5-hydroxymethylfurfural(11.09), 3,5-dimethoxytoluene(11.62), 3,4-dimethoxyphenol(12.87), 2-methyl-1,3-benzenediol(13.13), 2-methoxybenzyl alcohol(13.53), phenol,4-methoxy-3-(methoxymethyl)-(13.97), 3,4-dimethoxy-benzaldehyde(14.44), 1,6-anhydro-beta-d-glucopyranos(14.64), 2,5-dimethoxy-4-methylbenzaldehyde(15.43), 3-phenyl-2-propenal(15.49), 2-methylbutanedioic acid bis(1-methylpropyl) ester (15.59), hexanedioic acid bis(2-methylpropyl) ester(16.80), tetradecanoic acid(17.65), 1,2-benzenedicarboxylic acid bis(2-methylpropyl) ester(18.72), methyl 14-methylpentadecanoate(19.37), hexadecanoic acid(19.70), bis(2-ethylhexyl) maleate(21.39), squalene(26.80)

[a] The number in the bracket indicates the retention time of the compound, min.

unit, demethylation of cresols caused by the direct hydrogen-transfer and radical coupling mechanisms was another important source for phenol [36]. As the main products of the lignin pyrolysis process, 15 guaiacol-type compounds were detected in the volatile and among which guaiacol, 4-methyl guaiacol and 2-methoxy-4-vinylphenol accounted for a large proportion. Wherein CAL yielded the largest amount of this type of products, which meant guaiacyl unit in the CAL should be more abundant than the lignins extracted from the studied biomass. In contrast, the composition of the syringol type compounds was simple, nevertheless, the relative contents showed great differences. The amount of syringol type compounds from RHKL was only 1.6%, whereas it was up to 8.7% for RSKL. As presented in Fig. 5, the proportion of catechol type compounds was quite high for the pyrolysis volatiles of PSKL [35.0%] and CSKL [27.6%], which was far more than CAL [6.7%]. As shown in Fig. 8, hydroxycinnamic acid and ferulic acid, through their ether and ester bonds, served as the "bridge" between the lignin and polysaccharide fraction (mainly hemicellulose) [37,38]. They could easily undergo decarbonylation to form styrene and 4-hydroxy-3-methoxystyrene [39]. As demonstrated in Fig. 9, the total relative contents of styrene and 4-hydroxy-3-methoxystyrene were associated with the raw material type and could be generalized in the order of CLH, CHL, LCH type according to the classification in Fig. 2. For example, the total amounts of styrene and 4-hydroxy-3-methoxystyrene from WHSKL and CCKL were 4.5% and 5.5% (Table 2), respectively, which were much higher than those from other lignin samples. It indicated that there was a close relationship between the amount of styrene and 4-hydroxy-3-methoxystyrene from the lignin and the proportion of hemicellulose existed in its original biomass.

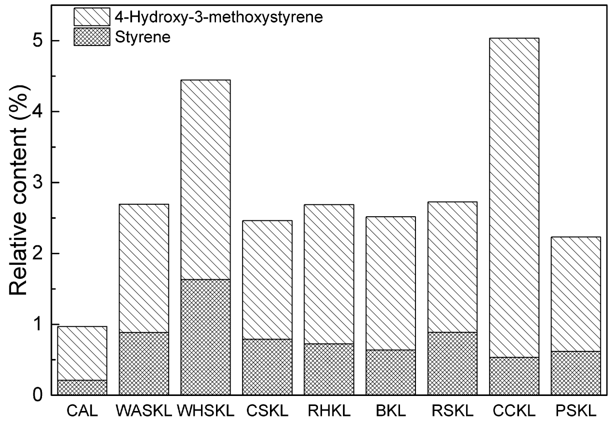

**Fig. 9.** Distributions of styrene and 4-hydroxy-3-methoxystyrene.

## 4. Conclusions

The pyrolysis characteristics of lignins extracted from eight agricultural residues were studied, and the conclusions can be drawn as follows:

- Pyrolysis behaviors of G, GS and HGS type lignins were different. The lignin type and H-abstraction reaction affected the charcoal residue greatly and the H unit in the non-woody lignin resulted in a more complicated pyrolysis behavior than the woody lignin.
- Peanut shell lignin and cotton stalk lignin were suitable for producing catechol type compounds.
- The amount of styrene and 4-hydroxy-3-methoxystyrene from lignin pyrolysis had an important link with the content of hemicellulose found in its original biomass.

## Acknowledgements

The authors appreciate greatly the financial support from the National Basic Research Program of China (2013CB228102), the National Natural Science Foundation of China (51376075), the Special Fund for Agro-scientific Research in the Public Interest(201303095), and the Foundation of State Key Laboratory of Coal

Combustion (FSKLCC1413). The experiment was also assisted by the Analytical and Testing Center at Huazhong University of Science & Technology (http://atc.hust.edu.cn). Mr. Ho Simon Wang has helped improve the linguistic presentation of the manuscript.

## References

[1] M.P. Pandey, C.S. Kim, Chem. Eng. Technol. 34 (2011) 29.
[2] A. Lourenço, J. Gominho, A.V. Marques, H. Pereira, Bioresour. Technol. 123 (2012) 296.
[3] E. Jakab, O. Faix, F. Till, J. Anal. Appl. Pyrolysis 40 (1997) 171.
[4] Q. Liu, S. Wang, Y. Zheng, Z. Luo, K. Cen, J. Anal. Appl. Pyrolysis 82 (2008) 170.
[5] X.J. Guo, S.R. Wang, K.G. Wang, Z.Y. Luo, Chem. Res. Chin. Univ. 27 (2011) 426.
[6] A.J. Ragauskas, G.T. Beckham, M.J. Biddy, R. Chandra, F. Chen, M.F. Davis, B.H. Davison, R.A. Dixon, P. Gilna, M. Keller, Science 344 (2014) 1246843.
[7] M. Zhang, F.L. Resende, A. Moutsoglou, D.E. Raynie, J. Anal. Appl. Pyrolysis 98 (2012) 65.
[8] P. De Wild, W. Huijgen, H. Heeres, J. Anal. Appl. Pyrolysis 93 (2012) 95.
[9] L. Chen, H. Chen, Q. Lu, Y. Song, X. Ding, X. Wang, H. Yang, CIESC J. 65 (2014) 8.
[10] J.C. del Riío, P. Prinsen, J. Rencoret, L. Nieto, J.S. Jimeínez-Barbero, J. Ralph, A.N.T. Martínez, A. Gutieírrez, J. Agric. Food Chem. 60 (2012) 3619.
[11] J.C. Del Río, J. Rencoret, P. Prinsen, A.N.T. Martínez, J. Ralph, A. Gutieírrez, J. Agric. Food Chem. 60 (2012) 5922.
[12] J. Rencoret, J. Ralph, G. Marques, A. Gutieírrez, A.N.T. Martínez, J.C. del Riío, J. Agric. Food Chem. 61 (2013) 2434.
[13] T. Ona, M. Shibata, K. Fukazawa, Tappi J. 78 (1995) 121.
[14] O. Faix, Holzforschung 45 (1991) 21.
[15] R.J. Sammons, Harper, P. David, Labbé, Nicole, BioResources 8 (2013) 2752.
[16] C.-M. Popescu, M.-C. Popescu, G. Singurel, C. Vasile, D.S. Argyropoulos, S. Willfor, Appl. Spectrosc. 61 (2007) 1168.
[17] H. Yang, R. Yan, H. Chen, D.H. Lee, C. Zheng, Fuel 86 (2007) 1781.
[18] A. Alves, M. Schwanninger, H. Pereira, J. Rodrigues, J. Anal. Appl. Pyrolysis 76 (2006) 209.
[19] J.C. del Rio, A. Gutiérrez, I.M. Rodríguez, D. Ibarra, A.T. Martinez, J. Anal. Appl. Pyrolysis 79 (2007) 39.
[20] D.K. Shen, S. Gu, K.H. Luo, S.R. Wang, M.X. Fang, Bioresour. Technol. 101 (2010) 6136.
[21] T. Ohra-aho, F.J.B. Gomes, J.L. Colodette, T. Tamminen, J. Anal. Appl. Pyrolysis 101 (2013) 166.
[22] Z. Wang, Q. Lu, X.F. Zhu, Y. Zhang, ChemSusChem 4 (2011) 79.
[23] D. Shen, S. Gu, K.S. Luo Wang, M. Fang, Bioresour. Technol. 101 (2010) 6136.
[24] M. Brebu, T. Tamminen, I. Spiridon, J. Anal. Appl. Pyrolysis 104 (2013) 531.
[25] O. Faix, E. Jakab, F. Till, T. Székely, Wood Sci. Technol. 22 (1988) 323.
[26] H. Kawamoto, S. Horigoshi, S. Saka, J. Wood Sci. 53 (2007) 168.
[27] T. Kotake, H. Kawamoto, S. Saka, J. Anal. Appl. Pyrolysis 104 (2013) 573.
[28] T. Kotake, H. Kawamoto, S. Saka, J. Anal. Appl. Pyrolysis 105 (2014) 309.
[29] J.-Y. Liu, S.-B. Wu, R. Lou, BioResources 6 (2011) 1079.
[30] S. Wang, K. Wang, Q.Y. Liu Gu, Z.K. Luo Cen, T. Fransson, Biotechnol. Adv. 27 (2009) 562.
[31] M. Asmadi, H. Kawamoto, S. Saka, J. Anal. Appl. Pyrolysis 92 (2011) 417.
[32] T. Hosoya, H. Kawamoto, S. Saka, J. Anal. Appl. Pyrolysis 83 (2008) 78.
[33] C. Xu, S. Hu, J. Xiang, L. Zhang, L.C. Sun Shuai, Q. Chen, L. He, E.M.A. Edreis, Bioresour. Technol. 154 (2014) 313.
[34] M. Asmadi, H. Kawamoto, S. Saka, In Zero-Carbon Energy Kyoto 2010, Springer, 2011, pp. p129.
[35] J. Hu, D. Shen, R. Xiao, S. Wu, H. Zhang, Energy Fuels 27 (2012) 285.
[36] M. Asmadi, H. Kawamoto, S. Saka, J. Anal. Appl. Pyrolysis 92 (2011) 76.
[37] G.C. Galletti, P. Bocchini, Rapid Commun. Mass Spectrom. 9 (1995) 815.
[38] B. Xiao, X. Sun, R. Sun, Polym. Degrad. Stab. 74 (2001) 307.
[39] M. Klein, P. Virk, Energy Fuels 22 (2008) 2175.